Brief communication

MOLECULAR METABOLISM

Notch intracellular domain overexpression in adipocytes confers lipodystrophy in mice

Dionysios V. Chartoumpekis [1,*], Dushani L. Palliyaguru [1], Nobunao Wakabayashi [1], Nicholas K.H. Khoo [1], Gabriele Schoiswohl [2], Robert M. O'Doherty [2], Thomas W. Kensler [1]

ABSTRACT

Objective: The Notch family of intermembrane receptors is highly conserved across species and is involved in cell fate and lineage control. Previous *in vitro* studies have shown that Notch may inhibit adipogenesis. Here we describe the role of Notch in adipose tissue by employing an *in vivo* murine model which overexpresses Notch in adipose tissue.

Methods: Albino C57BL/6J $Rosa^{NICD/NICD}$::Adipoq-Cre (Ad-NICD) male mice were generated to overexpress the Notch intracellular domain (NICD) specifically in adipocytes. Male $Rosa^{NICD/NICD}$ mice were used as controls. Mice were evaluated metabolically at the ages of 1 and 3 months by assessing body weights, serum metabolites, body composition (EchoMRI), glucose tolerance and insulin tolerance. Histological sections of adipose tissue depots as well as of liver were examined. The mRNA expression profile of genes involved in adipogenesis was analyzed by quantitative real-time PCR.

Results: The Ad-NICD mice were heavier with significantly lower body fat mass compared to the controls. Small amounts of white adipose tissue could be seen in the 1-month old Ad-NICD mice, but was almost absent in the 3-months old mice. The Ad-NICD mice also had higher serum levels of glucose, insulin, triglyceride and non-esterified fatty acids. These differences were more prominent in the older (3-months) than in the younger (1-month) mice. The Ad-NICD mice also showed severe insulin resistance along with a steatotic liver. Gene expression analysis in the adipose tissue depots showed a significant repression of lipogenic (Fasn, Acacb) and adipogenic pathways (C/ebpα, C/ebpβ, Pparγ2, Srebf1).

Conclusions: Increased Notch signaling in adipocytes in mice results in blocked expansion of white adipose tissue which leads to ectopic accumulation of lipids and insulin resistance, thus to a lipodystrophic phenotype. These results suggest that further investigation of the role of Notch signaling in adipocytes could lead to the manipulation of this pathway for therapeutic interventions in metabolic disease.

Keywords Notch; Adipocyte; Lipodystrophy; Insulin resistance; Lipogenesis; Adipogenesis

1. INTRODUCTION

Adipose tissue is an organ that stores excess energy in the form of fat and has endocrine properties manifested by the production and secretion of hormones such as leptin and adiponectin [1]. Adipose tissue has been studied mainly in the context of obesity and type 2 diabetes where white adipose tissue (WAT) expands so as to accommodate the surplus of energy intake. Accompanying this expansion, WAT inflammation and the secretion of inflammatory cytokines have been associated with the development and exacerbation of insulin resistance [2]. Limiting the expansion of WAT is of major importance since surplus lipids cannot be stored in the form of triglycerides; excess lipids then accumulate in ectopic sites such as liver and muscle, worsening insulin resistance [3].

The importance of the capacity and expandability of WAT becomes much more evident in the case of lipodystrophy. Lipodystrophy is a disorder characterized by selective loss of body fat and is accompanied by severe insulin resistance. A series of genetic lipodystrophies has been reported in humans and reflect mutations in genes such as *AGPAT2*, *BSCL2*, *CAV1*, *PTRF*, *CIDEC*, *PPARG* [4]. These genes are implicated in triglyceride synthesis, fusion of lipid droplets and adipogenesis. Although lipodystrophies are relatively rare diseases, there is an increased interest in the development of mouse models so as to better understand the pathophysiological mechanisms of lipodystrophy and the role of specific genes in adipose tissue functionality. Current mouse models are genetic knock-outs of *C/ebpa*, *Pparg*, *Agpat2*, *Cav1* or transgenic mice such as AZIP/F1 and ap2-*Srebp-1c* [5]. The usefulness of these mouse models lies not only in the fact that they can be used to understand the functions of specific genes but also can expand our understanding of the pathophysiology of insulin resistance [6].

In the present report, we describe a novel mouse model of lipodystrophy that arises from adipose tissue specific overexpression of the Notch intracellular domain (NICD). The Notch signaling pathway is highly conserved across species, playing roles in cellular differentiation, proliferation and apoptosis [7]. It consists of intermembrane receptors that can be bound by Notch ligands expressed on the surface of adjacent effector cells. This binding initiates the proteolytic cleavage of Notch by which NICD is released from the membrane, enters the

[1]Department of Pharmacology & Chemical Biology, School of Medicine, University of Pittsburgh, Pittsburgh, PA 15261, USA [2]Division of Endocrinology, Department of Medicine, University of Pittsburgh, Pittsburgh, PA 15261, USA

*Corresponding author. 200 Lothrop St, E1316 BST, Pittsburgh, PA 15261, USA. Tel.: +1 4126245854. E-mail: dic16@pitt.edu (D.V. Chartoumpekis).

Received April 6, 2015 • Revision received April 21, 2015 • Accepted April 24, 2015 • Available online 2 May 2015

http://dx.doi.org/10.1016/j.molmet.2015.04.004

nucleus to drive downstream signaling. Notch targets a number of genes, such as hairy and enhancer of split-1 (*Hes-1*), a prototypical target gene that encodes a transcriptional repressor [8].

Research on the role of the Notch pathway in the field of metabolism is relatively limited, focusing principally on the role of Notch in adipocyte differentiation using *in vitro* adipogenesis models such as 3T3-L1 cells [9,10]. Given that these studies were performed *in vitro* and taking into account recent studies on the protective effect of Notch inhibition in hepatocytes against fatty liver and insulin resistance [11,12], we investigated the role of Notch in the adipocyte by using a $Rosa^{NICD/NICD}$::Adipoq-Cre (Ad-NICD) mouse that overexpresses NICD specifically in adipose tissue as driven by the adiponectin promoter. We report herein that adipose-tissue specific overexpression of NICD results in a profound lipodystrophic, insulin resistant phenotype.

2. MATERIALS AND METHODS

2.1. Mice

All mouse experiments were performed at the University of Pittsburgh and were approved by the Institutional Animal Care and Use Committee. Gt(Rosa)26Sortm1(Notch1)Dam/J ($Rosa^{NICD/NICD}$) [13] and B6; FVB-Tg(Adipoq-cre)1Evdr/J [14] mice were obtained from Jackson Laboratories (Bar Harbor, ME). $Rosa^{NICD/NICD}$ mice were crossed with Adipoq-Cre mice and the male offspring $Rosa^{NICD/-}$::AdipoqCre were crossed with female $Rosa^{NICD/NICD}$ to get the desired phenotype of $Rosa^{NICD/NICD}$::AdipoqCre (Ad-NICD mice). Male Ad-NICD mice were mated with female $Rosa^{NICD/NICD}$ to generate the male mice used in the experiments.

$Rosa^{NICD/NICD}$, used as controls, and $Rosa^{NICD/NICD}$::AdipoqCre (Ad-NICD) were both in the albino C57BL/6J background. An experimental cohort of male mice was sacrificed at 1 month of age and another experimental cohort was sacrificed at 3 months of age. The 1-month old cohort included 8 control and 9 Ad-NICD male mice. The 3-month old cohort included 7 control and 6 Ad-NICD male mice. Another cohort (5 control and 8 Ad-NICD mice) was used to evaluate the growth curves of the mice starting from 22 days old until the age of 90 days. The genotyping primers as well as a more detailed description of the $Rosa^{NICD/NICD}$::AdipoqCre model can be found in the supplementary material. The mice were housed at 22 °C, 50% humidity with a 12 h light/dark cycle with *ad libitum* access to water and food (Prolab Isopro RMH 3000 5P76 irradiated diet, LabDiet, St Louis, MO).

2.2. Body fat composition and metabolic tests in mice

Body fat composition was assessed using NMR-MRI-based technology (EchoMRI, Houston, TX). Blood glucose was measured using a Precision Xtra glucose meter (Abbott, Chicago, IL) in blood collected from the tails of mice. Glucose tolerance was assessed by injecting intraperitoneally a single dose of D-glucose (1 g/kg) after a 16 h overnight fasting with free access to water. Insulin tolerance was assessed by injecting mice intraperitoneally with 0.75 units/kg insulin (Humalog, Eli Lilly, Indianapolis, IN) after a 4 h fasting with free access to water.

2.3. Serum metabolites

Blood was drawn under isoflurane anesthesia with cardiac puncture and was allowed to clot at room temperature for 30 min. Serum was collected after centrifuging the blood at 2000 × *g* for 30 min at 4 °C. Triglycerides and cholesterol concentrations were measured using a colorimetric and a fluorometric assay kit, respectively, from Cayman Chemical (Ann Arbor, MI). Liver triglycerides were also quantified using the same kit. Concentrations of non-esterified fatty acids were measured photometrically using the NEFA-HR kit (Wako Chemicals, Japan). Leptin and insulin were measured using ELISA kits from R&D systems (Minneapolis, MN) and Mercodia (Sweden), respectively.

2.4. Histology

Tissue was immersed in 10% formalin or in O.C.T. (Sakura, Torrance, CA) for the frozen sections. Hematoxylin and Eosin (H&E) stained sections were prepared by the Department of Pathology, University of Pittsburgh. Oil-red-O (ORO) staining of frozen sections was performed by fixing them in 10% formalin, then staining with ORO and after thorough washing, the slides were counterstained with hematoxylin. Photos were taken in a Leica DM5000B microscope.

2.5. RNA preparation and quantitative real-time PCR

Total RNA was prepared using Trizol (Life Technologies) and then a RNeasy kit followed by DNAse digestion (Qiagen, Valencia, CA). RNA quality and quantity was evaluated by electrophoresis and spectrophotometry at 260/280 nm prior to reverse transcriptase reaction. cDNA was synthesized with the qScript system (Quanta Biosciences, Gaithersburg, MD). Real-time PCR was performed on an iCycler-MyIQ (Biorad, Hercules, CA) with iQ SYBR green supermix (Biorad) in tetraplicate 20 µl reactions. The PCR efficiency was determined from standard curves and the Pfaffl method [15] was used for calculations of fold changes. The evaluation of the stability of the reference genes was performed using the genorm algorithm [16]. The geometric means of the two most stable reference genes were used to normalize the gene expression data. The primer pairs used for the real-time PCR as well as the results of the genorm algorithm for each reference gene are included in the supplemental data.

2.6. Statistical analysis

The Student's t-test was used to compare the control versus the Ad-NICD mice using Prism 5 for Windows (GraphPad Software, La Jolla, CA).

3. RESULTS

3.1. Ad-NICD mice are heavier with low body fat content

Comparisons of the body weights of male Ad-NICD mice with their $Rosa^{NICD/NICD}$ (control) counterparts indicate that they weigh significantly more at weaning (22 days of age) and that this difference in weight is accentuated over time (Figure 1A). The absolute amount of food consumption was higher in the Ad-NICD mice (Figure 1B), but when normalized to body weight, no significant difference was observed (Figure 1C). However, the absolute amounts of body fat were significantly ($p < 0.05$) lower in the Ad-NICD mice at 1-month of age (1.30 g vs 2.22 g in controls) (Figure 1D) and in 3-month old mice (2.97 g vs 5.87 g in controls) (Figure 1F), as measured by EchoMRI. The fat mass to body weight ratio was significantly lower in the Ad-NICD mice both at 1 and 3 months of age (Figure 1E,G). On the other hand, the Ad-NICD mice had increased absolute lean body mass at 1 and 3 months of age (Figure 1H,J) while the lean mass as % of body weight showed little difference (Figure 1I,K).

As is explicitly shown in the necropsy images of epididymal white adipose tissue (eWAT) in Figure 1L, the 1-month old Ad-NICD mice had minimal amounts of eWAT (0.09% BW vs 0.29% BW). H&E staining of the eWAT (Figure 1M) showed a greater amount of smaller adipocytes per optical field in the Ad-NICD mice (Supplementary Fig. S1B). This difference was not so pronounced in the inguinal white adipose tissue (iWAT). On the other hand, the interscapular brown adipose tissue (iBAT) was heavier (0.47% BW vs 0.33% in controls) and paler in color (Figure 1N). As evidenced by the H&E section of iBAT, this difference

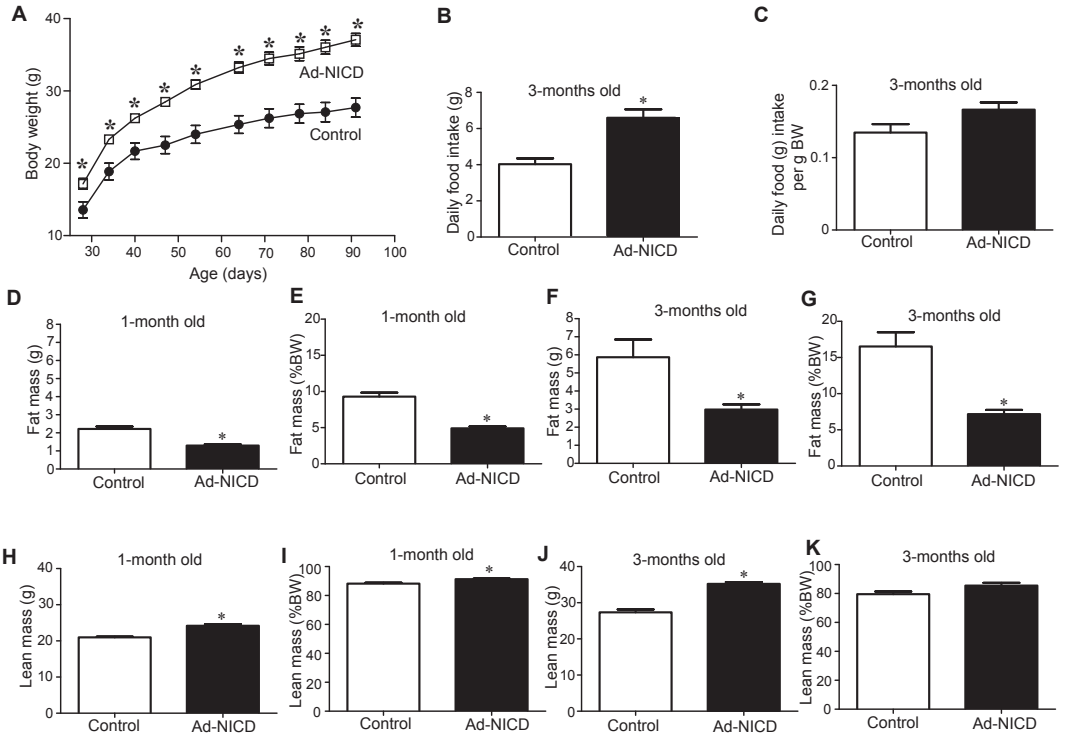

Figure 1: Phenotypic evaluation of the Rosa$^{NICD/NICD}$:: Adipoq-Cre (Ad-NICD) mouse. A. Body weight measurements in 22 day old to 90 day old male mice. Control mice are the Rosa$^{NICD/NICD}$. n = 5 for the control and n = 8 for the Ad-NICD. B. Daily food intake as assessed in single-housed mice (n = 5 for each genotype). C. Daily food intake expressed as grams per gram of body weight (BW). D.Absolute fat mass measurement using Echo-MRI in 1-month old male mice. n = 8 for the control and n = 9 for the Ad-NICD. E. Fat mass measurement using Echo-MRI expressed as percentage of the total body weight (%BW) in 1-month old male mice. n = 8 for the control and n = 9 for the Ad-NICD. F. Absolute fat mass measurement using Echo-MRI in 3-month old male mice. n = 7 for the control and n = 6 for the Ad-NICD. G. Fat mass measurement using Echo-MRI expressed as %BW in 3-month old male mice. n = 7 for the control and n = 6 for the Ad-NICD. H. Absolute lean mass measurement using Echo-MRI in 1-month old male mice. n = 8 for the control and n = 9 for the Ad-NICD. I. Lean mass measurement using Echo-MRI expressed as percentage of the total body weight (%BW) in 1-month old male mice. n = 8 for the control and n = 9 for the Ad-NICD. J. Absolute lean mass measurement using Echo-MRI in 3-month old male mice. n = 7 for the control and n = 6 for the Ad-NICD. K. Lean mass measurement using Echo-MRI expressed as %BW in 3-month old male mice. n = 7 for the control and n = 6 for the Ad-NICD. L. Necropsy photos of the epididymal white adipose tissue (eWAT) in 1-month old mice. Ruler values are in cm. The diagram shows the weight of the eWAT expressed as %BW. n = 8 for the control and n = 9 for the Ad-NICD. M. Representative microscope photos of hematoxylin & eosin stained paraffin embedded sections of epididymal (eWAT) and inguinal (iWAT) white adipose tissue from 1-month old male mice. N. Necropsy photos of interscapular brown adipose tissue (iBAT) from 1-month old male mice. Ruler values are in cm. The diagram shows the weight of the iBAT expressed as %BW. n = 8 for the control and n = 9 for the Ad-NICD. O. Representative microscope photos of hematoxylin & eosin stained paraffin embedded sections of interscapular brown adipose tissue (iBAT) from 1-month old male mice. Data show means ± SEM, *p < 0.05.

was probably due to the increased accumulation of lipids in the iBAT of the Ad-NICD mice in which iBAT contains much larger lipid droplets than in the control mice (Figure 1O).

3.2. Serum profiles of the Ad-NICD mice are consistent with diabetic lipodystrophy that exacerbates with age

Serum leptin levels were significantly lower in the Ad-NICD mice as expected since leptin is mainly produced by white adipocytes. There was a 2.5-fold difference in serum leptin levels in the 1-month old mice and this difference was substantially more pronounced in the 3-month old mice (28-fold) as shown in Table 1. The Ad-NICD mice also had higher starvation glucose levels and higher insulin levels, which is consistent with insulin resistance. The Ad-NICD mice had 7 and 36 times higher insulin levels than the control mice at 1and 3-months of age, respectively. This outcome indicates an insulin resistant phenotype that worsens with age. The lipid profile also reflected the low capacity of adipose tissue in the Ad-NICD mice; the Ad-NICD mice had higher triglyceride levels (1.7 fold in the 1-month old and 3.5 fold in the 3-month old mice). Cholesterol and non-esterified fatty acids levels were also higher in the Ad-NICD mice, especially in the older mice (Table 1).

3.3. Adipocyte-specific NICD overexpressing mice are insulin resistant and glucose intolerant

Intraperitoneal insulin tolerance tests (IPITT) unveiled an insulin resistant phenotype of the Ad-NICD mice, starting at least as early as 1-month of age and dramatically deteriorating with age as shown in the IPITT test in the 3-month old mice (Figure 2A,B). It is impressive that the 3-month old mice do not significantly decrease their glucose levels after injection with insulin until 90-minutes post-injection. The intraperitoneal glucose tolerance test (IPGTT) results did not differ between the two genotypes in the 1-month old mice (Figure 2A, right panel). This may indicate that while mice of this age are already insulin resistant, their higher serum insulin levels may be adequate to overcome the peripheral insulin resistance and to clear the glucose from their blood as effectively as the control mice. However, as the mice age, the insulin resistance increases and the subsequent, much higher levels of insulin that are secreted from the pancreas are no longer sufficient to overcome the peripheral insulin resistance (Figure 2B, right panel).

The H&E as well as the Oil-Red-O (ORO) stains of the liver sections indicate increased hepatic lipid accumulation that worsens with age (Figure 2C). This increased lipid accumulation is also evident by the

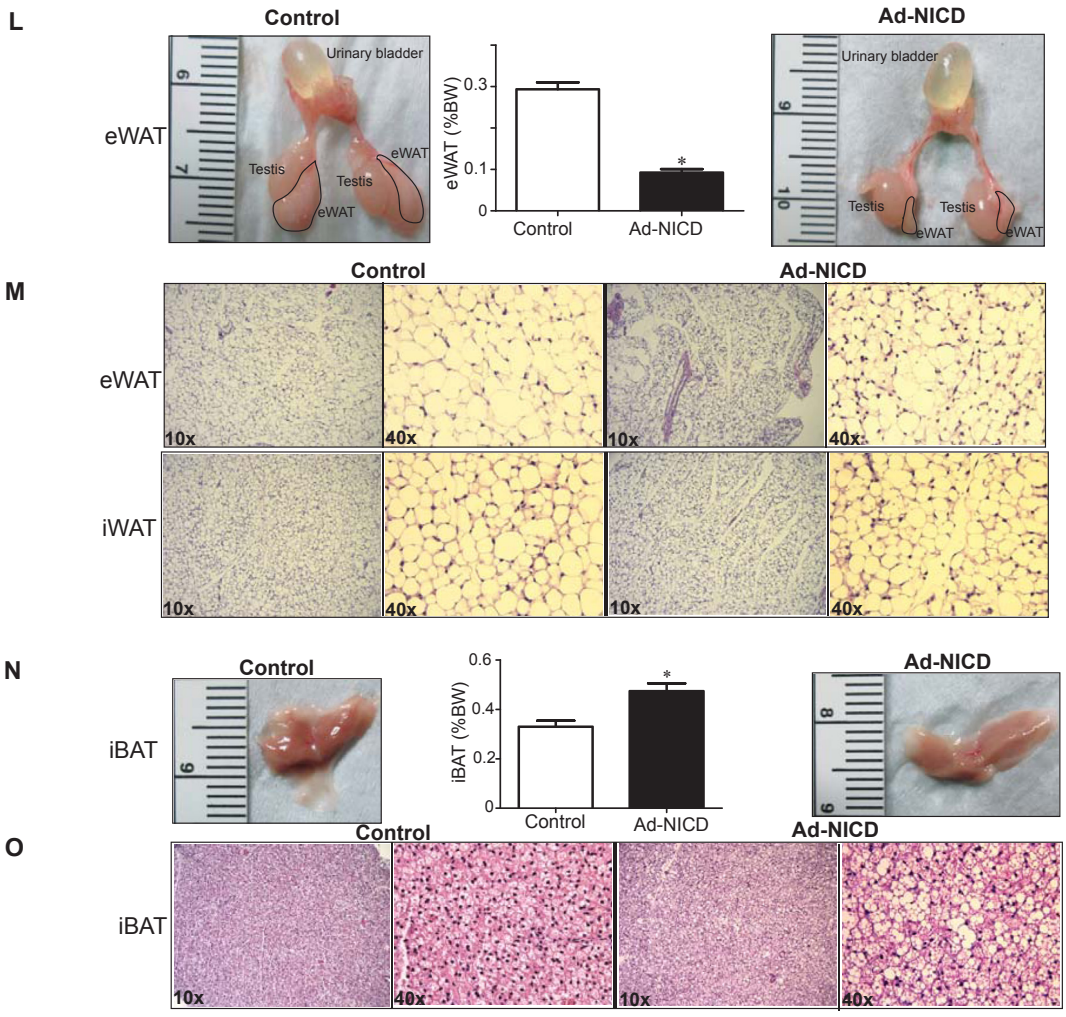

Figure 1: (*continued*).

gross presentation of the livers of the Ad-NICD mice at necropsy, their increased liver to body weight ratios and by their increased (almost 6-fold) triglyceride content (Figure 2D). The fatty liver phenotype was in accordance with the observed insulin resistance and could have been secondary to the diminished capacity of WAT in the Ad-NICD mice to expand and store excess energy in the form of fat.

3.4. Ad-NICD mice have a distinct transcriptional profile in adipose tissue

First, to confirm that *Hes1*, a prototypical target gene of the Notch pathway, is induced in the adipose tissues of adipocyte-specific NICD overexpressing mice, real-time quantitative PCR (qPCR) was used. Indeed, *Hes1* mRNA levels were induced 4-fold and 3-fold in the eWAT and iWAT of the Ad-NICD mice and 1.6-fold in the iBAT (Figure 3). Second, fatty acid synthase (*Fasn*), a rate-limiting enzyme of *de novo* lipogenesis (palmitate production from malonyl-CoA), was quantified by qPCR and was found to be extremely suppressed in eWAT (100 times) and in iWAT (10 times) of the Ad-NICD mice (Figure 3). Similarly, another enzyme of the *de novo* lipogenic pathway, acetyl-CoA carboxylase, which catalyzes the production of malonyl-CoA from acetyl-CoA, was significantly suppressed. As shown in Figure 3, mRNA levels of the isotype 2 of this enzyme (Acacb) were 10-times and 2-times lower in

Table 1 — Serum metabolites.

	1-month old		3-months old	
	Control	Ad-NICD	Control	Ad-NICD
Leptin (pg/ml)	4528 ± 547.6	1921 ± 190.1*	10110 ± 3244.0	364 ± 54.3*
Glucose (mg/dl)	132.9 ± 5.7	191.3 ± 17.5*	131.4 ± 6.8	201.5 ± 11.6*
Insulin (μg/l)	0.37 ± 0.05	2.41 ± 0.64*	0.74 ± 0.15	26.63 ± 6.80*
Cholesterol (mg/dl)	74.2 ± 8.2	91.6 ± 5.6	47.1 ± 5.0	70.6 ± 8.8*
Triglycerides (mg/dl)	41.7 ± 5.5	69.4 ± 7.1*	47.0 ± 3.8	161.5 ± 23.7*
NEFA (mEq/l)	0.30 ± 0.02	0.38 ± 0.03*	0.41 ± 0.02	0.76 ± 0.05*

n = 8 for the control and n = 9 for the Ad-NICD for the 1-month old male mice and n = 7 for the control and n = 6 for the Ad-NICD for the 3-month old male mice.
* $p < 0.05$ compared to the control genotype of the same age. Data are expressed as means ± SEM.

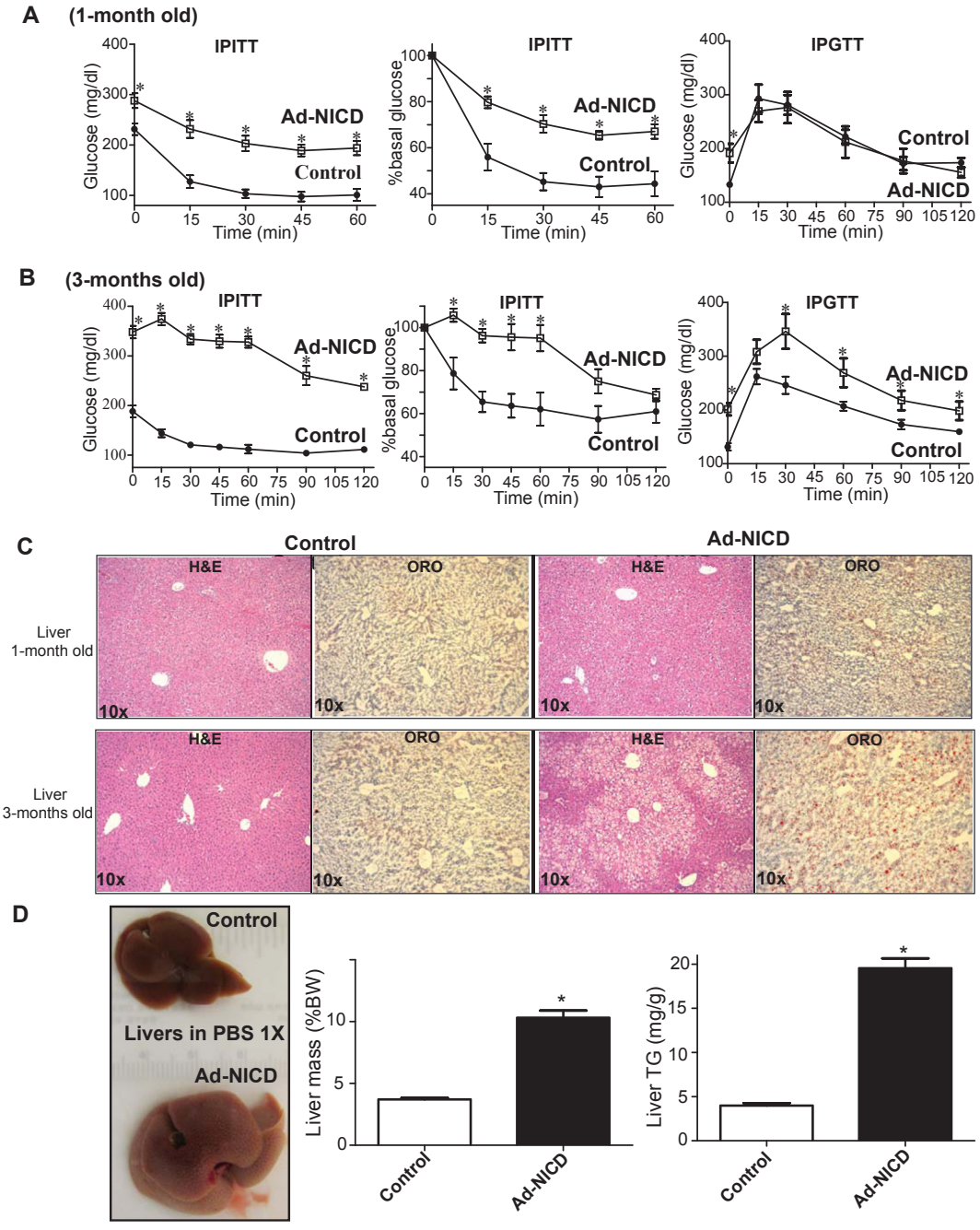

Figure 2: Assessment of insulin resistance in the Rosa$^{NICD/NICD}$.: Adipoq-Cre (Ad-NICD) mouse. A. Intraperitoneal insulin tolerance test (IPITT) in 1-month old male mice expressed as absolute glucose values (left panel) or as percentage of basal (time 0) glucose levels (middle panel). Intraperitoneal glucose tolerance test (IPGTT) in the same mice (right panel). n = 8 for the control and n = 9 for the Ad-NICD. B. Intraperitoneal insulin tolerance test (IPITT) in 3-month old male mice expressed as absolute glucose values (left panel) or as percentage of basal (time 0) glucose levels (middle panel). Intraperitoneal glucose tolerance test (IPGTT) in the same mice (right panel). n = 7 for the control and n = 6 for the Ad-NICD. C. Representative microscope photos of hematoxylin & eosin stained paraffin embedded sections and of oil-red-O (ORO) counterstained with hematoxylin frozen sections of liver from 1-month old and 3-month old male mice. D. Necropsy photo of livers from control and Ad-NICD 3-month old male mice immersed in PBS 1X (left panel). Liver mass of 3-month old male mice expressed as percentage of body weight (%BW)-middle panel. Total liver triglycerides measurement as mg per g of liver tissue. n = 7 for the control and n = 6 for the Ad-NICD. Data show means ± SEM, *p < 0.05.

the eWAT and the iWAT of the Ad-NICD mice, respectively, compared to controls. No difference was observed in the iBAT.

Given that serum leptin levels were decreased in the Ad-NICD mice, mRNA levels of leptin were quantified in adipose tissue, which is its major production site. eWAT of the Ad-NICD mice produced 6-times less leptin mRNA than the control mice; iWAT had 3-times less leptin mRNA whereas no difference was found in transcript levels of leptin in iBAT.

As the iWAT depot has the potential to undergo "browning", the expression levels of PR Domain Containing 16 (*Prdm16*), which regulates the "beige" adipocytes properties [17], were assessed. The Ad-NICD mice showed about 50% reduced *Prdm16* expression in iWAT (Figure 3). Moreover, the expression levels of 2 recently described cell surface markers of brown and "beige" adipocytes, proton assistant amino acid transporter-2 (*Pat2*) and Purinergic Receptor P2X Ligand-

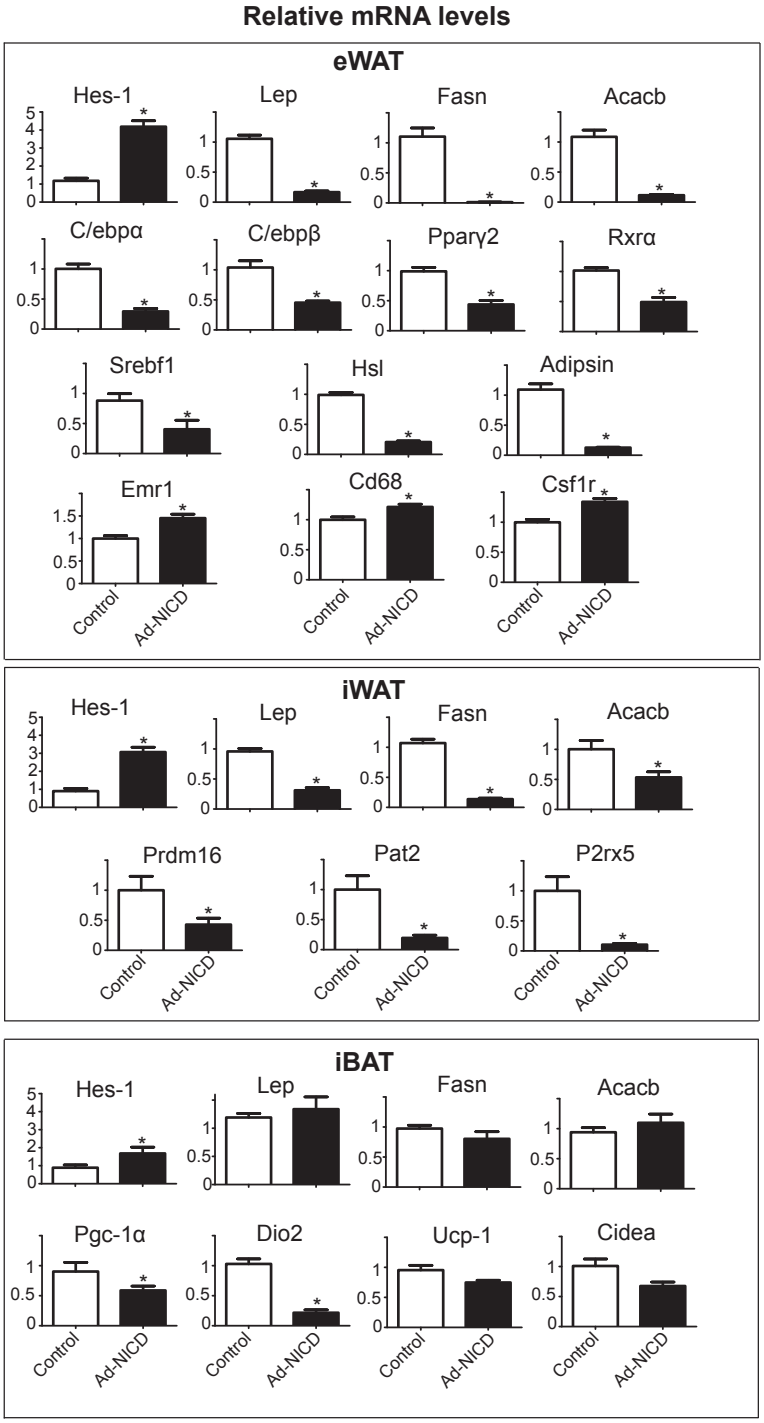

Figure 3: Relative mRNA levels of genes involved in metabolic processes in epididymal white adipose tissue (eWAT), inguinal white adipose tissue (iWAT) and interscapular brown adipose tissue (iBAT) from 1-month old male mice. Quantitative real-time PCR was used to assess these levels. More details about the selection of the reference genes and of the primers used can be found in the supplemental material. n = 8 for the control and n = 9 for the Ad-NICD. Data show means ± SEM, *$p < 0.05$. *Hes-1*; hairy and enhancer of split 1. *Lep*; leptin. *Fasn*; fatty acid synthase. *Acacb*; acetyl-CoA carboxylase 2. *C/ebpα*; CCAAT/enhancer binding protein α. *C/ebpβ*; CCAAT/enhancer binding protein β. *Pparγ2*; peroxisome proliferator-activated receptor γ2. *Rxrα*; retinoid X receptor α. *Srebf-1*; sterol regulatory element binding transcription factor 1. *Hsl*; hormone sensitive lipase. *Pgc-1α*; peroxisome proliferator-activated receptor gamma, coactivator 1α. *Dio2*; deiodinase, iodothyronine, type II. *Ucp-1*; uncoupling protein 1. *Cidea*; cell death-inducing DFFA-like effector a, *Emr1*; Egf-Like Module Containing, Mucin-Like, Hormone Receptor-Like 11, *Csf1r*; Colony Stimulating Factor 1 Receptor, *Prdm16*; PR Domain Containing 16, *Pat2*; proton assistant amino acid transporter-2, *P2rx5*; Purinergic Receptor P2X, Ligand-Gated Ion Channel 5.

Gated Ion Channel 5 (*P2rx5*) [18] were markedly reduced in the iWAT of the Ad-NICD mice (Figure 3). Hence, iWAT of Ad-NICD mice appears to contain less "beige" adipocytes compared to the control mice.

Expression of genes that control different stages of the highly regulated process of adipocyte differentiation, such as CCAAT-enhancer-binding proteins α and β (*C/ebp*α, *C/ebp*β), peroxisome proliferated activated receptor γ2 (*Ppar*γ*2*), retinoid X receptor α (*Rxr*α) and sterol regulatory element-binding transcription factor 1 (*Srebf-1*), were all reduced 50% or more in the eWAT of the Ad-NICD mice. This difference was not seen in the iWAT (Supplementary Fig. S2B). Another adipocyte marker, Adipsin, which is required for the synthesis of acylation stimulating protein to promote triglyceride synthesis and storage, was also reduced 8-fold in the Ad-NICD mice. Hormone-sensitive lipase (Hsl), which hydrolyzes tri-, di-, mono-glycerides as well as cholesteryl esters, had almost 5-times lower mRNA levels in the eWAT of the Ad-NICD mice. Lastly, the expression of macrophage markers Egf-Like Module Containing, Mucin-Like, Hormone Receptor-Like 1 (*Emr1*), Colony Stimulating Factor 1 Receptor (*Csf1r*) and *Cd68* were increased about 50% in the eWAT of the Ad-NICD mice (Figure 3) indicating increased macrophages infiltration.

To better assess the phenotype of the lipid laden brown adipocytes of the Ad-NICD mice, mRNA levels of peroxisome proliferator-activated receptor γ coactivator 1-α (*Pgc-1*α), type II iodothyronine deiodinase (*Dio2*), uncoupling protein 1 (*Ucp-1*) and cell death-inducing DFFA-Like Effector A (*Cidea*) were quantified in the iBAT. *Pgc-1*α levels were half that of the control mice while *Dio2* levels were 5-times less abundant in the Ad-NICD mice. *Ucp-1* and *Cidea* consistently trended towards reduced levels in the Ad-NICD mice without reaching statistical significance.

4. DISCUSSION

In the present work we report a new lipodystrophy model by genetically enhancing the Notch signaling pathway in adipocytes. The diabetic lipodystrophic phenotype was apparent at 1 month of age and became exacerbated with time. This model shares common features, such as insulin resistance, diabetes, fatty liver, dyslipidemia and low leptin levels, with previously described mouse lipodystrophy models [5]. The increased daily food consumption (Figure 1B) and the ectopic accumulation of lipids in the liver resulting in hepatomegaly (Figure 2D), can at least partially explain the increased body weights of the Ad-NICD mice.

It is interesting that the leptin levels of the 3-month old Ad-NICD mice are much lower (6-times) than the levels of the 1-month old mice of the same genotype and account for the enhanced fold difference of serum leptin levels between the control and the Ad-NICD mice that increases with age. Thus, leptin secretion is compromised with age in these mice. Given that adipose tissue is the major source of leptin and that eWAT becomes harder to detect in the 3-month old mice (Supplementary Fig. S1A), two possible scenarios warrant further investigation: i. the eWAT adipocytes of AdNICD mice have lost their ability to expand (hypertrophy) and ii. the eWAT cannot induce *de novo* adipogenesis (hyperplasia). To better approach these alternative hypotheses, the recent "AdipoChaser" mouse model can be useful [19]. This mouse model can be used to track *de novo* adipogenesis *in vivo* by detecting β-gal negative cells. One of the major insights from this mouse model was that gonadal adipocytes differentiate postnatally while subcutaneous adipocytes are more committed to differentiate as early as embryonic days 14–18. In the adult mouse the gonadal adipose tissue has a very limited potential for *de novo* adipogenesis in contrast with the subcutaneous adipose tissue. Therefore, this information indicates that the diminished eWAT (gonadal WAT) in the Ad-NICD mice is likely a result of postnatal development and that the main defect in eWAT adipocytes might reflect a diminished potential to expand (hypertrophy). A cross of the AdipoChaser mouse with the Ad-NICD mouse would certainly give more definite insights.

To ensure that the observed differences in the eWAT and in the iWAT of the Ad-NICD mice are not due to different expression of NICD in these 2 depots, the expression of *NICD* and of *Egfp* was assessed (Supplementary Fig. S2C). It is evident that the NICD levels are the same in these 2 depots and the expression of *Egfp*, that is derived solely from the Rosa 26 locus driven transgene expression (Supplementary Fig. S1C), also shows no difference. Moreover, the fact that the WAT is almost totally diminished in the older (3-months) Ad-NICD mice (Supplementary Fig. S1A) could indicate that adipocytes can be led to necrotic death or apoptosis [20] and are not replenished by the differentiation of preadipocytes to mature adipocytes due to the enhanced Notch signaling. The transcriptional profiling of the WAT of the Ad-NICD mice revealed an extreme down-regulation of key enzymes involved in *de novo* lipogenesis (*Fasn*, *Acacb*). This suppression of lipogenesis could be one of the contributing factors to the resultant lipodystrophic phenotype. When the lipogenic potential of adipocytes is diminished, excess energy cannot be stored in the white adipocytes in the form of lipids. Thus, increased circulation of lipids and their ectopic accumulation result in insulin resistance. This role of adipocyte lipogenesis has become evident also from studies where lipogenesis is activated and leads to an ameliorated metabolic phenotype [21].

A series of markers of adipocyte differentiation including *Ppar*γ*2*, *Rxr*α, *C/ebp*α, *C/ebp*β as well as *Srebf-1* were also found to be decreased in the eWAT of Ad-NICD mice. As noted before, the different transcription profile between eWAT and iWAT in the Ad-NICD may be due to a differential effect of NICD in different developmental stages (eWAT develops mainly postnatally while iWAT starts developing during embryonic days 14–18). Moreover, it is possible that *Hes-1*, which acts as a transcriptional repressor can mediate at least some of these effects. *Hes-1* has been described as a transcriptional repressor during adipogenesis in 3T3L1 preadipocytes [22] by acting, for example, in the promoter region of *Fasn* which is recognized by *Srebf-1*. In other work [23], Hes-1 has been described to repress *Ppar*γ transcriptional activity. Hence Hes-1 can potentially act as a transcriptional repressor for a series of adipocyte differentiation promoting transcription factors. This view is also supported by a study that showed that Hes-1 overexpression in 3T3-L1 preadipocytes inhibited their differentiation to adipocytes [9].

Last but not least, the increased lipid accumulation that is observed in the iBAT of the Ad-NICD mice can be explained by increased uptake of lipids from the blood, as happens in the liver. Moreover, the decreased expression of the well-described brown adipocyte markers *Pgc-1*α, *Dio2* and the trend for decreased *Ucp-1* and *Cidea* expression in the iBAT of Ad-NICD can contribute to the resulting phenotype.

Two recent studies hinted at a role for Notch in these adipose tissue properties. First, adipose tissue stem cells derived from visceral WAT depots of rats have an activated Notch pathway and a decreased capacity to differentiate to adipocytes whereas those derived from subcutaneous depots have decreased Notch signaling and higher adipogenic potential [24]. Second, Notch inhibition promotes browning of WAT and protects from obesity in mice by inducing *Pgc-1*α and *Prdm16* [25]. While our work was in progress, these investigators also generated Ad-NICD mice and showed that these mice are less glucose tolerant, more insulin resistant and show less energy expenditure and oxygen consumption than controls. This phenotype was attributed to the lower expression of genes that promote browning of WAT in their

iWAT, which was also confirmed in our study by the lower expression of *Prdm16*, *P2rx5* and *Pat2* genes in iWAT. However, herein we report for the first time that the overexpression of NICD in adipose tissue confers lipodystrophy in the Ad-NICD mice that can directly explain the diabetic phenotype of these mice even on a regular diet.

5. CONCLUSIONS

In conclusion, the present work paves the way for future studies on the role of Notch pathway in the development and expansion of adipose tissue. This new lipodystrophy model can be further used to study the role of Notch in the development of the various adipose tissue depots and unveil new Notch interactions with adipogenic and metabolic pathways. Pharmacological manipulation of the Notch pathway specifically in adipose tissue could be an attractive option to enhance the capacity of adipocytes in the setting of obesity and type 2 diabetes.

CONFLICT OF INTEREST

No conflicts of interest to disclose.

AUTHOR CONTRIBUTIONS

DVC, DLP and GS performed experiments. DVC, NW and TWK designed experiments. DLP, NW, NKK, GS, RMO contributed to discussion. DVC and TWK wrote the paper. TWK supervised the study.

ACKNOWLEDGMENTS

Financial support by National Institutes of Health grant CA94076 (to TWK). DVC is supported by a Marie Curie International Outgoing Fellowship (PIOF-GA-2012-329442) within the 7th European Community Framework Programme. GS was supported by Erwin Schrödinger Fellowship-J3221-B19 funded by Austrian Science Fund (FWF).

APPENDIX A. SUPPLEMENTARY DATA

Supplementary data related to this article can be found at http://dx.doi.org/10.1016/j.molmet.2015.04.004.

REFERENCES

[1] Kershaw, E.E., Flier, J.S., 2004. Adipose tissue as an endocrine organ. Journal of Clinical Endocrinology and Metabolism 89(6):2548—2556.

[2] Lumeng, C.N., Saltiel, A.R., 2011. Inflammatory links between obesity and metabolic disease. Journal of Clinical Investigation 121(6):2111—2117.

[3] Virtue, S., Vidal-Puig, A., 2010. Adipose tissue expandability, lipotoxicity and the metabolic syndrome—an allostatic perspective. Biochimica et Biophysica Acta 1801(3):338—349.

[4] Garg, A., 2011. Clinical review#: Lipodystrophies: genetic and acquired body fat disorders. Journal of Clinical Endocrinology and Metabolism 96(11):3313—3325.

[5] Savage, D.B., 2009. Mouse models of inherited lipodystrophy. Disease Models & Mechanisms 2(11—12):554—562.

[6] Asterholm, I.W., Halberg, N., Scherer, P.E., 2007. Mouse models of lipodystrophy key reagents for the understanding of the metabolic syndrome. Drug Discovery Today Disease Models 4(1):17—24.

[7] Guruharsha, K.G., Kankel, M.W., Artavanis-Tsakonas, S., 2012. The Notch signalling system: recent insights into the complexity of a conserved pathway. Nature Reviews Genetics 13(9):654—666.

[8] Jarriault, S., Brou, C., Logeat, F., Schroeter, E.H., Kopan, R., Israel, A., 1995. Signalling downstream of activated mammalian Notch. Nature 377(6547):355—358.

[9] Ross, D.A., Rao, P.K., Kadesch, T., 2004. Dual roles for the Notch target gene Hes-1 in the differentiation of 3T3-L1 preadipocytes. Molecular and Cellular Biology 24(8):3505—3513.

[10] Garces, C., Ruiz-Hidalgo, M.J., Font de Mora, J., Park, C., Miele, L., Goldstein, J., et al., 1997. Notch-1 controls the expression of fatty acid-activated transcription factors and is required for adipogenesis. Journal of Biological Chemistry 272(47):29729—29734.

[11] Pajvani, U.B., Shawber, C.J., Samuel, V.T., Birkenfeld, A.L., Shulman, G.I., Kitajewski, J., et al., 2011. Inhibition of Notch signaling ameliorates insulin resistance in a FoxO1-dependent manner. Nature Medicine 17(8):961—967.

[12] Pajvani, U.B., Qiang, L., Kangsamaksin, T., Kitajewski, J., Ginsberg, H.N., Accili, D., 2013. Inhibition of Notch uncouples Akt activation from hepatic lipid accumulation by decreasing mTorc1 stability. Nature Medicine 19(8):1054—1060.

[13] Murtaugh, L.C., Stanger, B.Z., Kwan, K.M., Melton, D.A., 2003. Notch signaling controls multiple steps of pancreatic differentiation. Proceedings of the National Academy of Sciences of the United States of America 100(25):14920—14925.

[14] Eguchi, J., Wang, X., Yu, S., Kershaw, E.E., Chiu, P.C., Dushay, J., et al., 2011. Transcriptional control of adipose lipid handling by IRF4. Cell Metabolism 13(3):249—259.

[15] Pfaffl, M.W., 2001. A new mathematical model for relative quantification in real-time RT-PCR. Nucleic Acids Research 29(9):e45.

[16] Vandesompele, J., De Preter, K., Pattyn, F., Poppe, B., Van Roy, N., De Paepe, A., et al., 2002. Accurate normalization of real-time quantitative RT-PCR data by geometric averaging of multiple internal control genes. Genome Biology 3(7). RESEARCH0034.

[17] Cohen, P., Levy, J.D., Zhang, Y., Frontini, A., Kolodin, D.P., Svensson, K.J., et al., 2014. Ablation of PRDM16 and beige adipose causes metabolic dysfunction and a subcutaneous to visceral fat switch. Cell 156(1—2):304—316.

[18] Ussar, S., Lee, K.Y., Dankel, S.N., Boucher, J., Haering, M.F., Kleinridders, A., et al., 2014. ASC-1, PAT2, and P2RX5 are cell surface markers for white, beige, and brown adipocytes. Science Translational Medicine 6(247):247ra103.

[19] Wang, Q.A., Tao, C., Gupta, R.K., Scherer, P.E., 2013. Tracking adipogenesis during white adipose tissue development, expansion and regeneration. Nature Medicine 19(10):1338—1344.

[20] Sun, K., Kusminski, C.M., Scherer, P.E., 2011. Adipose tissue remodeling and obesity. Journal of Clinical Investigation 121(6):2094—2101.

[21] Cao, H., Gerhold, K., Mayers, J.R., Wiest, M.M., Watkins, S.M., Hotamisligil, G.S., 2008. Identification of a lipokine, a lipid hormone linking adipose tissue to systemic metabolism. Cell 134(6):933—944.

[22] Ross, D.A., Hannenhalli, S., Tobias, J.W., Cooch, N., Shiekhattar, R., Kadesch, T., 2006. Functional analysis of Hes-1 in preadipocytes. Molecular Endocrinology 20(3):698—705.

[23] Herzig, S., Hedrick, S., Morantte, I., Koo, S.H., Galimi, F., Montminy, M., 2003. CREB controls hepatic lipid metabolism through nuclear hormone receptor PPAR-gamma. Nature 426(6963):190—193.

[24] Ferrer-Lorente, R., Bejar, M.T., Badimon, L., 2014. Notch signaling pathway activation in normal and hyperglycemic rats differs in the stem cells of visceral and subcutaneous adipose tissue. Stem Cells and Development 23(24):3034—3048.

[25] Bi, P., Shan, T., Liu, W., Yue, F., Yang, X., Liang, X.R., et al., 2014. Inhibition of Notch signaling promotes browning of white adipose tissue and ameliorates obesity. Nature Medicine 20(8):911—918.

